

# Oxygen distribution in packed bed membrane reactors for partial oxidation systems and the effect on the product selectivity

**Citation for published version (APA):**

Kurten, U., Sint Annaland, van, M., & Kuipers, J. A. M. (2004). Oxygen distribution in packed bed membrane reactors for partial oxidation systems and the effect on the product selectivity. *International Journal of Chemical Reactor Engineering*, 2, A24-1/27. Article A24.

**Document status and date:**

Published: 01/01/2004

**Document Version:**

Publisher's PDF, also known as Version of Record (includes final page, issue and volume numbers)

**Please check the document version of this publication:**

- A submitted manuscript is the version of the article upon submission and before peer-review. There can be important differences between the submitted version and the official published version of record. People interested in the research are advised to contact the author for the final version of the publication, or visit the DOI to the publisher's website.
- The final author version and the galley proof are versions of the publication after peer review.
- The final published version features the final layout of the paper including the volume, issue and page numbers.

[Link to publication](#)

**General rights**

Copyright and moral rights for the publications made accessible in the public portal are retained by the authors and/or other copyright owners and it is a condition of accessing publications that users recognise and abide by the legal requirements associated with these rights.

- Users may download and print one copy of any publication from the public portal for the purpose of private study or research.
- You may not further distribute the material or use it for any profit-making activity or commercial gain
- You may freely distribute the URL identifying the publication in the public portal.

If the publication is distributed under the terms of Article 25fa of the Dutch Copyright Act, indicated by the "Taverne" license above, please follow below link for the End User Agreement:

[www.tue.nl/taverne](http://www.tue.nl/taverne)

**Take down policy**

If you believe that this document breaches copyright please contact us at:

[openaccess@tue.nl](mailto:openaccess@tue.nl)

providing details and we will investigate your claim.

# INTERNATIONAL JOURNAL OF CHEMICAL REACTOR ENGINEERING

---

*Volume 2*

2004

*Article A24*

---

## **Oxygen Distribution in Packed Bed Membrane Reactors For Partial Oxidation Systems and its Effect On Product Selectivity**

U. Kuerten\*

Martin van Sint Annaland†

J.A.M. Kuipers‡

\*University of Twente, u.kuerten@ct.utwente.nl

†Twente University, m.v.sintannaland@tue.nl

‡University of Twente, J.A.M.Kuipers@ct.utwente.nl

ISSN 1542-6580

Copyright ©2004 by the authors.

All rights reserved. No part of this publication may be reproduced, stored in a retrieval system, or transmitted, in any form or by any means, electronic, mechanical, photocopying, recording, or otherwise, without the prior written permission of the publisher, bepress, which has been given certain exclusive rights by the author.

# Oxygen Distribution in Packed Bed Membrane Reactors For Partial Oxidation Systems and its Effect On Product Selectivity

U. Kuerten, Martin van Sint Annaland, and J.A.M. Kuipers

## Abstract

Packed bed membrane reactors (PBMRs) are currently considered for the distributive addition of oxygen in partial oxidation systems. Among other advantages the decreased oxygen concentrations in the PBMR can result in improved product selectivities for reaction systems in which the oxygen dependency of the target product formation is less pronounced than that of the waste product formation. Oxidative dehydrogenation (ODH) of methanol to formaldehyde (Diakov et al., 2002) and ethylbenzene to styrene (Shakhnovich et al., 1984) are industrially relevant examples of such a kinetic system.

To achieve considerable selectivity improvements the oxygen concentration should be kept small compared to hydrocarbon concentrations. However, a decrease of the oxygen concentration is accompanied with a decrease in the effectiveness of the catalyst particles since the intraparticle oxygen concentration gradients (and not the hydrocarbon concentration gradients) predominantly determine the actual activity and product selectivities of the catalyst, rendering the common effectiveness factors inapplicable for the modeling of a PBMR.

Furthermore, concentration profiles over the radius of the packed bed can emerge, if the radial mass transport rate of oxygen from the membrane wall to the center of the bed is insufficient compared to the local oxygen consumption rate. If the transmembrane flux is dominated by convective transport as typical with porous membranes, the radial oxygen concentration profiles result in increased product losses, and the use of a one-dimensional reactor model may result in an overestimation of the product selectivity.

In this paper the effect of limitations of the oxygen mass transport in a PBMR – i.e. intraparticle and from the membrane to the centerline of the packed bed –

have been discussed for the ODH of methanol and ethylbenzene.

**KEYWORDS:** Membrane reactors, distributive feeding, oxidative dehydrogenation, modelling

## 1 INTRODUCTION

Membrane reactors are studied for a wide range of applications for e.g. yield enhancement of equilibrium-limited reactions via selective withdrawal of one of the products, selectivity enhancement by controlled dosing of one of the reactants and many other reasons (see e.g. Saracco et al., 1999 and the references listed there). Different types of membrane reactors can be distinguished (Hsieh, 1996): membrane reactors with catalytic active membranes or with a packed catalyst bed, membrane reactors for the selective removal of a reaction product (e.g. dehydrogenation with hydrogen removal) or for the distributive feeding of a reactant (e.g. partial oxidation with controlled oxygen feeding), membrane reactors with selective or porous membranes.

In heterogeneously catalyzed partial oxidation systems distributive feeding of oxygen via porous membranes and the thus realized low oxygen concentrations can significantly enhance the product selectivity, provided that the reaction order in oxygen for the formation of the target product is lower than the reaction order in oxygen for the formation of waste products. A decrease in the oxygen concentration is beneficial for the product selectivity for both consecutive and parallel reaction schemes. If the waste product is formed via a consecutive reaction, the reactor must possess low back-mixing characteristics in order to limit product losses. A packed bed membrane reactor (PBMR) combines the features of distributive oxygen feeding and low axial back-mixing of a packed bed reactor.

In the PBMR air or oxygen permeates through the membrane due to pressure or concentration gradients. From the membrane surface the oxygen penetrates into the packed bed perpendicular to the main flow direction of the reaction mixture (see Figure 1), and radial concentration profiles may emerge. These concentration profiles can influence the performance of the PBMR.

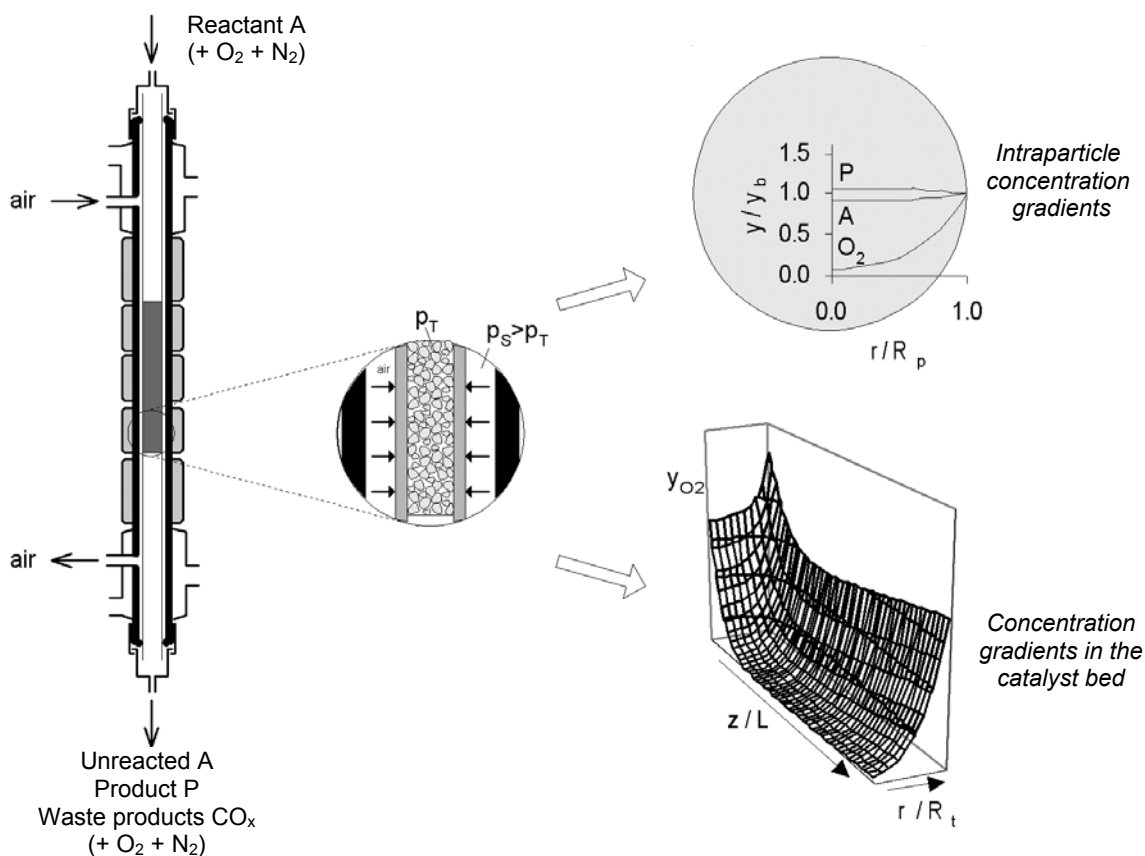


Figure 1. Schematic drawing of a packed bed membrane reactor illustrating the concentration gradients caused by mass transport limitations inside the catalyst particle and from the membrane wall to the center of the catalyst bed.

In addition, intraparticle transport limitations can play an important role, since often in these reactors porous catalysts are employed. However, the standard approach of effectiveness factors cannot be applied for this special type of reaction system. Due to the fact that oxygen is consumed in both reactions the particle effectiveness factors of the main and consecutive reactions are correlated. Thus, even if the consecutive reaction rate is small, the effectiveness factor of this reaction can be decreased by the consumption of oxygen by the primary reaction. The consecutive reaction could even be stronger effected by oxygen concentration gradients than the primary reaction due to the higher reaction order in oxygen. While in usual consecutive reactions of the type  $A \rightarrow B \rightarrow C$  the selectivity of the intermediate product is negatively influenced by intraparticle mass transport limitations, the reaction systems discussed in this paper show a selectivity improvement, if the oxygen concentration is small compared to the concentrations of the hydrocarbons, as is the case in the PBMR.

Two industrially important partial oxidation systems that can benefit from distributive feeding of oxygen are the oxidative dehydrogenation (ODH) of the ethylbenzene to styrene and the ODH of methanol to formaldehyde. These two reaction systems are analyzed in this paper concerning the benefits of distributive oxygen feeding and the effects of insufficient distribution of oxygen due to mass transfer limitations inside the particle and from the membrane surface to the center of the packed bed, using detailed reactor models for the PBMR. Firstly, these reactor models will be described and subsequently the effects of mass transfer limitations on the PBMR performance will be investigated with these models for the ODH of ethylbenzene and methanol respectively.

## 2 MODEL DESCRIPTION

Two models were developed for the evaluation of the effects of the two different types of mass transport limitation: a one-dimensional, heterogeneous model to investigate intraparticle effects and a two-dimensional, pseudo-homogeneous model for the transport effects from the membrane surface to the center of the packed bed.

A detailed description of the oxygen transport through the membrane is not included in this work. Here, the membrane is considered as an ideal distributor with a fixed membrane flow, independent from the reaction conditions inside the packed bed. This assumption enables an independent discussion of the influence of the oxygen distribution on the performance of the PBMR. For the same reason, possible heat effects were ignored in this paper. The temperature rise in a PBMR is strongly reduced compared to a fixed bed reactor (FBR) with completely premixed feed. This is an effect of both a better distribution of the reactivity over the length of the packed bed and an overall decreased activity due to the lower oxygen concentrations. Furthermore, a temperature runaway, a typical problem of the FBR with premixed feed, is less likely or even impossible in a PBMR, because the local oxygen consumption is limited by the transmembrane flow. Despite the fact that temperature effects are still relevant for assessing the true benefits of PBMRs, they will be ignored in this paper to focus on the discussion of mass transfer effects.

### 2.1 One-dimensional, heterogeneous PBMR model

To study the effect of intraparticle transport limitations on the performance of PBMRs a model describing the mass transport from the gaseous bulk to the particle surface and the intraparticle transport was developed. Obviously, the performance of the PBMR also depends on the overall design, as for example the tube diameter, the radial flow pattern (mainly determined by the particle to tube ratio) or the pressure drop over the length of the packed bed. To clearly elucidate the effects of the intraparticle diffusion limitations on the integral reactor performance these effects have been ignored here and are investigated separately with a two-dimensional model described in section 2.2. To facilitate the discussion of the effects also a constant and uniform distribution of the secondary flow has been assumed.

#### MODEL ASSUMPTIONS:

##### 1. One-dimensional plug flow model

The equations of change for the gas phase are based on the assumption of a one-dimensional plug flow model (Westerterp et al., 1984) neglecting the axial dispersion and the pressure drop of the packed bed. Source terms of the component continuity equations are due to mass transfer between the bulk of the gas phase and the catalyst surface, and the secondary mass flow. Homogeneous gas phase reactions have not been considered here.

Having neglected the pressure drop, the evaluation of the momentum balance is not required, since the local mass flow rate can be calculated a priori from the premixed mass flow and the part of the distributive flow that has been added via the membrane up to the given location, where uniform distribution of the distributive flow over the membrane length has been assumed if not mentioned otherwise.

### 2. Macro-porous, symmetrical catalyst particle

The catalyst particles are assumed to be of spherical shape and constant diameter  $d_p$ , so that a one-dimensional model can be used to describe the profiles inside the catalyst particle. The catalyst structure is assumed to be macro-porous, so that transport mechanisms like Knudsen diffusion can be neglected. It is assumed that the component mass transport inside the particle can be described by Fick's law of diffusion due to the relatively low concentrations of the relevant components.

The resulting model equations with the constitutive equations for the transmembrane flux and interphase mass transport have been listed in Table 1. At the reactor inlet and outlet the standard Danckwerts' boundary conditions (Westerterp et al., 1984) have been used for the gas phase mass balance, while symmetry at the particle center and continuity of the mass fluxes at the particle outer surface have been applied for the catalyst phase.

Table 1. Model equations for the one-dimensional, heterogeneous PBMR model.

Gas phase mass balance	Boundary conditions
$\frac{\partial}{\partial t}(\varepsilon \rho_g \omega_i) = -\frac{\partial}{\partial z}(\varepsilon \rho_g \omega_i v_z) - a n_{s,i} + \phi_{m,distr,i}$	$v_z \rho_g \omega_{i,0} = v_z \rho_g \omega_i \Big _{z=0}$
	$\frac{\partial \omega_i}{\partial z} \Big _{z=L} = 0$
Catalyst phase mass balance	Boundary conditions
$\frac{\partial}{\partial t}(\rho_g \omega_i) = \frac{1}{r^2} \frac{\partial}{\partial r} \left( r^2 D_{eff,i} \rho_g \frac{\partial \omega_i}{\partial r} \right) + S_i$	$\frac{\partial \omega_i}{\partial r} \Big _{r=0} = 0$
$S_i = M_i \sum_{j=1}^{nr} v_{ij} r_j$	$D_{eff,i} \rho_g \frac{\partial \omega_i}{\partial r} \Big _{r=R} = n_{s,i}$
Transmembrane flux	Interphase mass transport
$\phi_{m,distr,i} = \frac{\Phi_{m,distr} \omega_{distr,i}}{(\pi/4) d_i^2 L}$	$n_{s,i} = \rho_g k_{s,i} (\omega_i - \omega_{s,i})$

The molecular diffusion coefficients were estimated with the equation proposed by Wilke (1950) using the binary diffusion coefficients estimated by the empirical relation given by Fuller et al. (1966) (see Appendix A). In the calculation of the effective diffusion coefficient a ratio of the particle porosity and tortuosity  $\varepsilon/\tau = 0.15$  was assumed.

The steady-state solutions for the mass balances in the bulk of the gas phase and for the catalyst phase were obtained by solving the equations with accumulation terms using a finite difference technique. The two partial differential equations have been solved sequentially, where the equations were coupled via the concentrations and concentration gradients at the particle outer surface.

Typically 100 equidistant axial grid cells for the gas phase mass balance were used, whereas typically 50 cells on the particle radius with grid refinement towards the catalyst surface were used to solve the catalyst phase mass balance, with which grid-independent solutions were obtained.

## 2.2 Two-dimensional, pseudo-homogeneous PBMR model

In order to investigate the influence of radial profiles of the oxygen and hydrocarbons concentrations on the integral performance of the PBMR a two-dimensional, pseudo-homogeneous reactor model was developed. Often, a one-dimensional model is sufficiently accurate in describing the packed bed reactor, at least if temperature effects are small. In case of the PBMR, however, it is likely that a radial oxygen profile is established. If the PBMR is operated at a low oxygen concentration level with small axial concentration gradients over the length of the reactor, the local oxygen balance is (due to the high conversion rate) mainly determined by radial transport, which moreover is mainly dominated by dispersive transport driven by concentration gradients.

### MODEL ASSUMPTIONS:

#### 1. Pseudo-homogeneous reactor model

Axi-symmetry is assumed for the PBMR. Mass transfer limitations from the gas bulk to the catalyst surface and inside the catalyst particle have been ignored. The reaction rates can thus be described as a direct function of the gas phase concentrations. Furthermore, the structure of the packing is characterized by the bed porosity. Although the bed porosity can be a function of the radial position in the tube depending on the diameters of the catalyst particles and the membrane tube, here the bed porosity was assumed to be radially constant. A radial porosity profile, possibly important for cases with a low aspect ratio of the tube-to-particle diameters, can be easily included in the model, but the effects on the conversion and selectivity for an industrial scale PBMR were found to be very small (Kürten, 2003).

#### 2. Diffusive and dispersive transport can be described with a standard dispersion model (SDM)

It is assumed that gas phase mass transport in the PBMR can be modeled with a two-dimensional model for the convective flow with superimposed radial and axial dispersion.

Firstly, the flow model (gas phase total continuity and Navier-Stokes equations) is described, where after the component mass balances are given.

### 2.2.1 Flow model

The two-dimensional PBMR model calculates the gas phase velocity field by solving the total continuity and momentum equations (Brinkman, 1947) for the gas phase given respectively by:

$$\frac{\partial(\varepsilon\rho_g)}{\partial t} + \nabla \cdot (\varepsilon\rho_g\bar{v}) = 0 \quad \text{and} \quad (1)$$

$$\frac{\partial}{\partial t}(\varepsilon\rho_g\bar{v}) + \nabla \cdot (\varepsilon\rho_g\bar{v}\bar{v}) = -\varepsilon\nabla p - \beta\varepsilon\rho_g\bar{v} - \nabla \cdot (\varepsilon\bar{\tau}_g) + \varepsilon\rho_g\bar{g} \quad (2)$$

where

$$\text{- Friction coefficient: } \beta = 150 \frac{(1-\varepsilon)^2}{\varepsilon^3} \frac{\mu_g}{\rho_g d_p^2} + 1.75 \frac{1-\varepsilon}{\varepsilon^3} \frac{\varepsilon|\bar{v}|}{d_p} \quad (\text{Ergun's equation}) \quad (3)$$

$$\text{where } |\bar{v}| = \sqrt{v_r^2 + v_z^2}$$

$$\text{- Newtonian fluid: } \bar{\tau}_g = -\left(\lambda_g - \frac{2}{3}\mu_g\right)(\nabla \cdot \bar{v})\bar{I} - \mu_g \left[ (\nabla\bar{v}) + (\nabla\bar{v})^T \right] \quad (4)$$

$\lambda_g$  is the contribution of the bulk viscosity of the gas to the normal stress, which can be neglected for low-density gases (Bird et al., 1960).



$$\text{- Ideal gas law: } \rho_g = \frac{pM_g}{RT_g} \quad (5)$$

Although the physical properties (especially density and viscosity) are determined by the local composition, which are affected by the chemical reactions, the component mass balances are solved sequentially after having solved the flow model. This decoupling is possible and desired because of the large differences in time scales on which the hydrodynamic phenomena and chemical reactions take place. Furthermore, the decoupling has the clear advantage that different time steps and scales can be used when only the steady-state solutions are of interest, speeding up the calculations tremendously.

The total continuity and Navier-Stokes equations are solved with a finite difference technique on a staggered computational mesh (Patankar, 1980) using a first order time discretisation and implicit treatment of the pressure gradient and linearized implicit treatment of the drag forces. The implicit treatment of the pressure gradient term requires solving a pressure correction equation (Poisson equation) derived from the mass defect of the gas phase continuity equation. The convection terms have been discretised using a first order upwind scheme (Patankar, 1980), while the dispersion terms have been discretised with standard second order finite difference representations. Thus the sequence of computations is as follows:

For each new time step, firstly the density field is calculated from the old pressure and concentration field data using the ideal gas law. Subsequently, the velocity field is calculated using the discretised momentum equations, followed by the calculation of the new pressure field using the pressure correction equation. Then, the density field is updated using the equation of state and the iteration-loop is repeated until all variables have converged.

### 2.2.2 Component mass balances

The radial and axial concentration profiles in the PBMR are calculated from component mass balances accounting for two-dimensional convective and dispersive transport including a non-linear source term:

$$\frac{\partial \rho_g \varepsilon \omega_i}{\partial t} = -\frac{1}{r} \frac{\partial r \rho_g \varepsilon v_r \omega_i}{\partial r} - \frac{\partial \rho_g \varepsilon v_z \omega_i}{\partial z} + \frac{1}{r} \frac{\partial}{\partial r} \left( \rho_g D_{r,i} r \frac{\partial \omega_i}{\partial r} \right) + \frac{\partial}{\partial z} \left( \rho_g D_{z,i} \frac{\partial \omega_i}{\partial z} \right) + S_i \quad (6)$$

Here  $\omega_i$  represents the mass fractions of all components but one. The concentration of the component present in excess is calculated from the equation:  $\sum_{i=1}^{nc} \omega_i = 1$  (7)

In Equation (6)  $D_{r,i}$  and  $D_{z,i}$  represent the effective radial and axial dispersion coefficients, whereas the source terms are given by:  $S_i = (1 - \varepsilon) \rho_{cat} M_i \sum_{j=1}^{nrr} v_{ij} r_j$  (8)

Despite the addition of a distributive convective flow via the membrane tube wall, dispersion is the main driving force for radial transport. Correlations given in literature for the radial dispersion coefficient often sum the contributions by molecular diffusion and turbulent mixing (Tsotsas and Schlünder, 1988; Gunn, 1987).

$$D_r = D_r^m + D_r^t \quad (9)$$

The following correlation for the dispersion in the core of the packed bed was proposed by Tsotsas and Schlünder (1988):

$$D_r = (1 - \sqrt{1 - \varepsilon_0}) D_i^m + \frac{u_0 d_p}{PE_\infty (d_t / d_p \rightarrow \infty) f(d_t / d_p)} \quad (10)$$

where  $d_p$  is the particle diameter and  $d_t$  the tube diameter,  $PE_\infty (d_t / d_p \rightarrow \infty)$  is the limiting value of the Péclet number in an unconfined bed, which is about 8, and  $f(d_t / d_p)$  is a correction factor accounting for the influence of the tube wall and the resulting flow maldistribution. Near the tube wall the porosity of the bed and consequently the gas velocity is increased, so that in the bed center the velocity is below the average. This results in a lower axial dispersion in the core of the bed.

$$D_r' = \frac{u_0 d_p}{8 \left( 2 - \left( 1 - 2 \left( d_p / d_t \right) \right)^2 \right)} \quad \text{or} \quad D_r' = \frac{u_c d_p}{8} \quad (11), (12)$$

where  $u_0$  represents the average superficial velocity. Alternatively, the superficial velocity in the core of the bed  $u_c$  can be used, which avoids the correction term. The correlations presented above were derived from measurements, where a tracer was injected at the axis of the tube. In most cases the profiles did not reach the tube wall. So, the dispersion was determined in an area of nearly constant porosity and velocity profiles. Therefore, the equations are based on average values of the velocity and bed porosity, and do not include radial dependencies. In case of a membrane reactor, however, the oxygen is added through the membrane wall influencing the velocity field. Near the wall the gas velocity is distinctly higher than in the core, and therefore the influence of the radius on the dispersion was included.

$$D_r = (1 - \sqrt{1 - \varepsilon}) D_i^m + \frac{ud}{8} \quad (13)$$

where the local values are used for the superficial velocity. For the axial dispersion coefficient the same correlation was used, however with a 4 times larger contribution of the turbulent dispersion. Applying the correlations of Tsotsas and Schlünder (1988) allows an adjustment of the dispersion coefficient to the local gas velocity. In the present paper a radially constant porosity was assumed.

Table 2. Boundary and initial conditions for component mass balances.

	component mass balance
Left $r=0$	$\left. \frac{\partial \bar{\omega}}{\partial r} \right _{r=0} = 0$
Right $r=d_t/2$	$-(D_{r,i} \rho_g)_{nr+1/2} \left. \frac{\partial \omega_i}{\partial r} \right _{r=d_t/2} + (v_r \rho_g \varepsilon \bar{\omega}) \Big _{r=d_t/2} = \Phi_{m,distr,i} / (\pi d_t L)$
Bottom $z=0$	$-D_{z,i} \rho_g \left. \frac{\partial \omega_i}{\partial z} \right _{z=0} + (v_z \rho_g \varepsilon \omega_i)_{z=0} = \Phi_{m,0,i} / (\pi d_t^2 / 4)$
Top $z=L$	$\left. \frac{\partial \omega_i}{\partial z} \right _{z=L} = 0$
Initial $t=0$	$\omega_i(r, z) = \omega_{i,0}$

Again, a finite difference technique is used to discretise the equations employing the same computational mesh as used in the flow model. Convection is discretised with first order upwind, and for the diffusion terms standard second order central differences were used. The *alternating direction implicit* (ADI) method (Press et al., 1989) was applied, where a full time step is calculated via two half time steps, treating the transport in the radial

direction implicitly and in the axial direction explicitly in the first half step and vice versa in the next half time step. The gas phase physical properties have been modeled following Reid et al. (1988) using pure component properties of the data set of AIChE Design Institute for Physical Property Data. The usual Danckwerts-type boundary conditions have been implemented. Boundary and initial conditions have been summarized in Table 2.

### 2.2.3 Combination of the flow model and the reaction balance

Since only the steady state profiles are of interest here, the flow solver is advanced for 5 consecutive time steps, after which the reaction model is solved with a time step up to 1000 times larger than the time step used in the flow solver.

In the next sections the above-described models will be used to study the effects of mass transfer limitations on the performance (conversion and selectivity) of PBMRs for the oxidative dehydrogenation (ODH) of ethylbenzene and methanol.

## 3 OXIDATIVE DEHYDROGENATION OF ETHYLBENZENE

Styrene is industrially produced mainly in a two-step process by first alkylating benzene with ethene to form ethylbenzene, which is then dehydrogenated to styrene. Due to thermodynamic limitations only moderate ethylbenzene conversions can be achieved in this conventional process. This problem has been largely overcome in the commercial 'SMART' process by the sequential combustion of the hydrogen via selective catalytic oxidation. Thus ethylbenzene conversions of about 80 % can be achieved at a styrene selectivity of about 95 %.

As an alternative technique the oxidative dehydrogenation has been proposed (see e.g. the review article of Cavani and Trifirò, 1995b), which however suffers from undesired combustion reactions resulting in too low product selectivities. Two concepts can be followed in order to improve the product yield both as a combination of catalyst and reactor development.

Firstly, the development of a redox-type oxide catalyst. Lattice oxygen is expected to be selective, while surface oxygen is held responsible for undesired combustion reactions. The unselective oxygen could be avoided by separation of oxidative dehydrogenation with lattice oxygen and the re-oxidation of the catalyst. Watzenberger et al. (1999) discuss the unsteady-state oxidative dehydrogenation in a fixed bed reactor. The reactor cycle comprises of the ODH, the re-oxidation of catalyst and two intermediate periods of flushing with nitrogen. They claimed that the redox-catalyst achieved in lab-scale experiments selectivities of about 95 % at a total conversion of approximately 97 %. Yet, the economic feasibility of this process alternative depends on the oxygen load of the catalyst (8 g active oxygen / kg catalyst = 53 g styrene / kg catalyst) and the cycle times, which determine the required amount of catalyst, i.e. the size of the reactor.

The second reactor concept, the packed bed membrane reactor with distributive oxygen feeding, requires a catalyst for which the reaction order in oxygen for the formation of the target product is smaller than that for the waste product. For the demonstration of the potential of this concept for the ODH of ethylbenzene, reaction kinetics were taken from the literature. Shakhnovich et al. (1984) investigated the kinetics of the ODH of ethylbenzene on a zinc oxide modified vanadia/magnesia catalyst in the presence of steam. They investigated the catalyst in the steady state after the initial coke formation.

The following parallel-consecutive scheme for the main products was proposed:

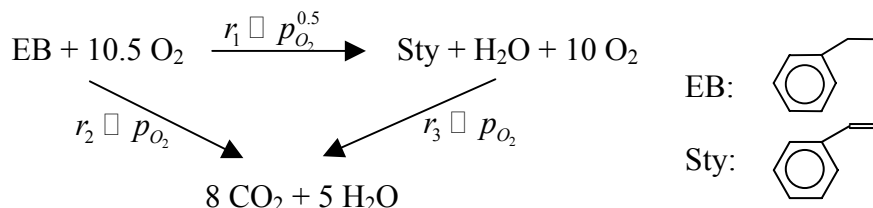


Figure 2. Model reactions for the ODH of ethylbenzene on a zinc oxide modified vanadia/magnesia catalyst by Shakhnovich et al. (1984).

The kinetics were studied for the following ranges of experimental conditions:

- Reaction temperature: 420 to 550°C,
- Initial ethylbenzene (EB) concentration  $p_{C_8H_{10},0}$ : 4.2 to 11.2 kPa,
- Initial oxygen concentration  $p_{O_2,0}$ : 4.4 to 9.6 kPa,
- Added steam  $p_{H_2O,0}$ : 10 to 80 kPa.

Table 3. Reaction kinetics by Shakhnovich et al. (1984).

$r_i$ [mol / g s]	$r_1 = K_I \frac{P_{C_3H_{10}} P_{O_2}^{0.5}}{B}$	$r_2 = K_{II} \frac{P_{C_3H_{10}} P_{O_2}}{B}$	$r_3 = K_{III} \frac{P_{C_3H_8} P_{O_2}}{B}$
$K_I$ [mol / g s kPa <sup>1+n</sup> ]	$4.91 \cdot 10^{-2} \exp(-7100/T)$	$6.55 \cdot 10^{-4} \exp(-7050/T)$	$4.55 \cdot 10^{-3} \exp(-7550/T)$
	$B = \left[ \left( 1 + k_1 p_{C_8H_{10}} + k_2 p_{C_8H_8} + k_3 p_{O_2} \right) \left( 1 + x \frac{P_{C_8H_{10}}}{P_{O_2}^{0.5}} \right) \right]^2$ with $x=0.04 \text{ kPa}^{-0.5}$		
$k_i$ [kPa <sup>-1</sup> ]	$2.31 \cdot 10^{-5} \exp(6300/T)$	$6.72 \cdot 10^{-5} \exp(6300/T)$	$2.62 \cdot 10^{-3} \exp(2500/T)$

In Figure 3a the influence of the oxygen concentration on the selectivity-conversion-plot is demonstrated for FBRs with premixed oxygen feeding and idealized PBMRs with an axially constant oxygen concentration. For the model calculations a reaction temperature of 550°C, an initial ethylbenzene mole fraction of  $y_{EB}=0.1$  and a flow rate of 100 ml/min were selected. The figure clearly demonstrates that the ODH of ethylbenzene with *premixed oxygen feeding* cannot compete with the standard dehydrogenation process and even less with the SMART process.

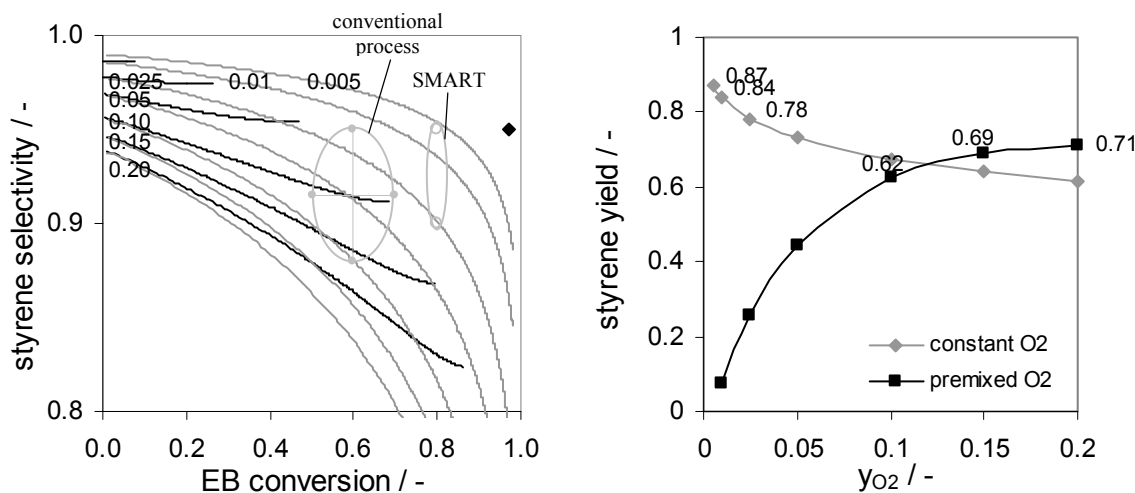


Figure 3. Influence of the oxygen concentration on (a) the styrene selectivity as a function of the EB conversion, (b) the styrene yield at 550°C. The EB mole fraction for all cases is  $y_{EB} = 0.1$  while that of oxygen is varied from  $y_{O_2} = 0.005$  to 0.2. The bold lines represent the model results for premixed oxygen, the thin lines for constant oxygen concentrations. In (a) the performance of the conventional, the SMART process and the unsteady-state oxidation process by Watzenberger et al. (1999) (diamond) are indicated.

The SMART process (conversion of 80 % at a selectivity of 95 %) has been considered as a target for the investigation of the PBMR. The yield of the SMART process is exceeded by a PBMR with a constant oxygen concentration of  $y_{O_2}=0.025$  (Figure 3b), but at a low styrene selectivity of only 84 %. Because of the high feed stock costs, such a low selectivity should be avoided. Thus an oxygen concentration of  $y_{O_2}=0.005$  is required. For a catalyst mass of 1.13 g a selectivity of 95.4 % is achieved at 80 % conversion, corresponding to a WHSV of 1.75 kg styrene produced per kg catalyst per hour. Additional model calculations at 500°C showed a small effect of the reaction temperature on the selectivity-conversion-plot. In this case 3.17 g catalyst was required to achieve a conversion of 80 % and a selectivity of 95.5 %.

Subsequently, the PBMR was not modeled with a constant oxygen concentration, but with a flow of air equally distributed over the length of the reactor. For an increased catalyst mass of 1.5 g the oxygen in premixed and distributive flow was optimized for maximum styrene yield under the constraint of a minimum styrene selectivity of 95 %. The (flat) maximum in the styrene yield was found for an inlet oxygen concentration of  $y_{O_2}=0.02$  of the premixed flow of  $\Phi_{V,0}=100$  ml/min and a distributive flow of  $\Phi_{V,air,distr}=35$  ml/min with a conversion of 85.4 % and a selectivity of 95.1 %.

In the following sections the effect of intraparticle mass transfer limitations and the transport from the membrane to the core of the packed bed on the PBMR performance will be studied with these optimized model parameters. Thereby, the feed flows and the catalyst mass are increased by a factor of 960 to simulate a membrane tube of industrial scale.

### 3.1 Intraparticle transport

In Table 4 the model parameters have been listed used for the evaluation of the influence of intraparticle mass transport limitations on the performance of a PBMR for the ODH of ethylbenzene to styrene, using the one-dimensional- heterogeneous model.

The effective diffusion coefficients of ethylbenzene and styrene are smaller than that of oxygen, and thus relatively strong concentration profiles for the hydrocarbons emerge in the catalyst particles. The ratio of the effective diffusion coefficients of ethylbenzene and oxygen was estimated (for a mixture of ethylbenzene, oxygen and nitrogen with  $y_{EB}=0.1$  and  $y_{O_2}=0.01$ ; see Appendix A) as:

$$\frac{D_{eff,EB}}{D_{eff,O_2}} = \frac{1 - y_{EB}}{1 - y_{O_2}} \frac{y_{EB} + 0.357 y_{N_2}}{y_{O_2} + 0.965 y_{N_2}} = 0.44 \quad (14)$$

Table 4. Model parameters for the study of the effects of intraparticle mass transfer limitations for the ODH of ethylbenzene.

Catalyst mass	$m_{cat}$	1.44-2.88 kg
Catalyst density	$\rho_{cat}$	1000 kg / m <sup>3</sup>
Particle diameter	$d_p$	1, 3, 5 mm
Interphase mass transfer coefficient	$k_s$	1 m / s
Reactor pressure and temperature	$p, T$	1.013 bar, 550 K
Premixed feed:	volumetric flow	$\Phi_{V,0}$ 5.76 m <sup>3</sup> (STP) / h
	mole fraction of reactant A	$y_{EB,0}$ 0.1
	mole fraction of oxygen	$y_{O_2,0}$ 0.02
Distributed feed:	volumetric flow	$\Phi_{V,distr}$ 2.016 m <sup>3</sup> (STP) / h
	mole fraction of oxygen	$y_{O_2,distr}$ 0.2

STP: 1.013 bar and 298 K

#### 3.1.1 Increase of the particle size

In Figure 4 and Figure 5 the influence of intraparticle mass transfer limitations on the reactor performance is shown for the particle diameters 1, 3 and 5 mm. While the effect is negligible for the smallest particle size, the relative loss in the styrene yield increases from 4 % to 10 % for 3 and 5 mm respectively.

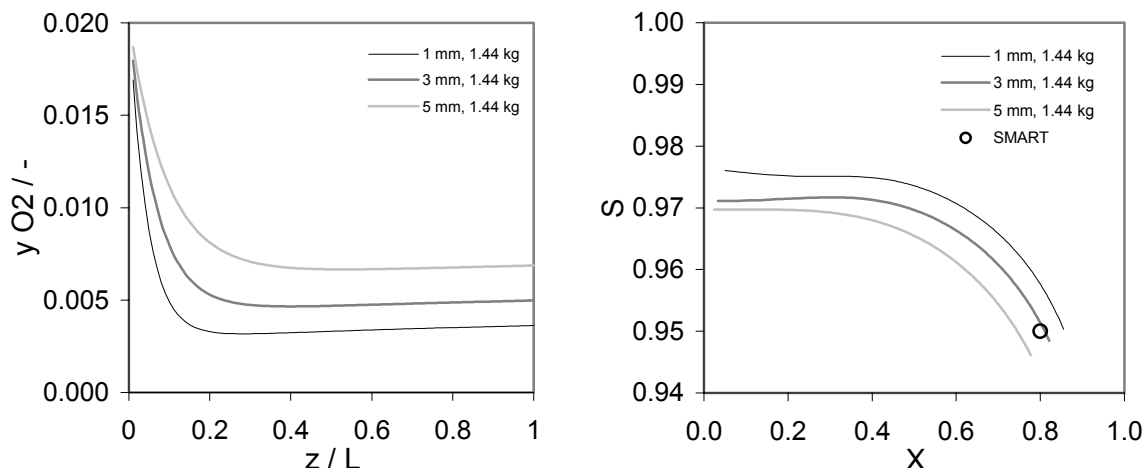


Figure 4. Influence of the particle size on the (a) the axial oxygen concentration profile and (b) selectivity – conversion – plot.

Because all reactions consume oxygen and because of the fact that the concentration gradients of oxygen in the particle are the strongest, the effectiveness of the different reactions are correlated and the usual approach to use a pseudo-homogeneous reactor model with effectiveness factors accounting for intraparticle mass transport limitations cannot be applied. For this reaction system, only the effectiveness factor for the oxygen consumption can be approximated using a modified Thiele modulus:

$$\phi' = \frac{d_p}{6} \sqrt{\frac{\left(\frac{0.5+1}{2} 0.5 r_1 + \frac{1+1}{2} (10.5 r_2 + 10 r_3)\right) \rho_{cat}}{D_{eff,O_2} (p_{O_2}/RT)}} \quad (15)$$

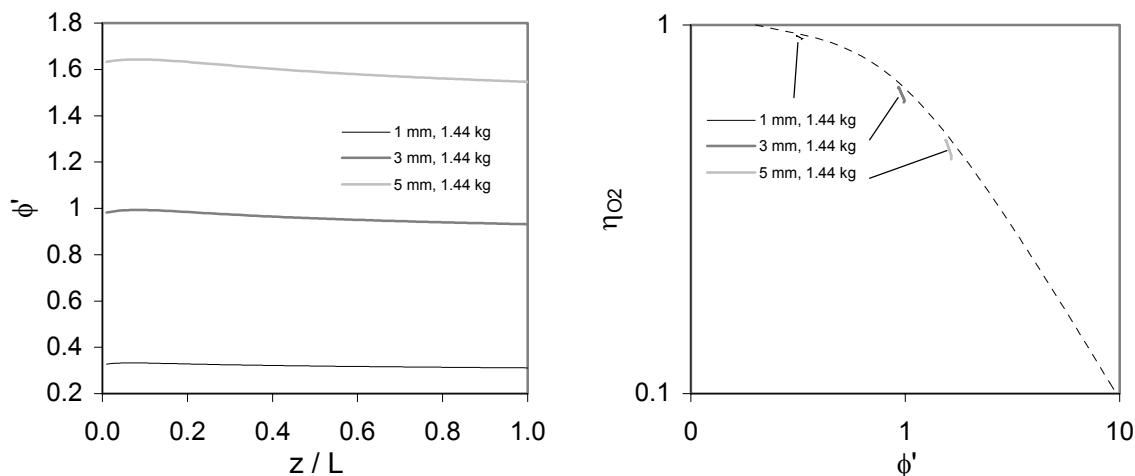


Figure 5. (a) Axial profile of the modified oxygen Thiele-modulus for different particle sizes and (b) particle effectiveness as a function of the Thiele-modulus (the dashed line represents equation (16)).

The particle effectiveness for the oxygen consumption can then be approximated by

$$\eta_{O_2} = \frac{1}{3\phi'^2} \left( \frac{3\phi'}{\tanh(3\phi')} - 1 \right) \quad (16)$$

which is the analytical solution for a single, first order reaction (Bird, Steward, Lightfoot, 1960). Figure 5b shows that the actual particle effectiveness is slightly lower than predicted with equation (16) which can be attributed to the effect of gradients in the hydrocarbon concentrations.

Yet, the effect of intraparticle mass transport limitations on the formation of styrene or carbon dioxide cannot be correlated to a single parameter.

The intrinsic effect of intraparticle mass transfer limitations on the product selectivity is illustrated in this paper in terms of the selectivity towards the waste product ( $1-\sigma$ ).

$$F_{1-\sigma} = \frac{\text{actual selectivity loss of catalyst particle}}{\text{selectivity loss corresponding to bulk concentrations}} \quad (17)$$

A selectivity factor  $F_{1-\sigma} > 1$  indicates that the product losses due to undesired combustion reactions is increased by the intraparticle mass transport limitations. Generally, the intraparticle gradients of the hydrocarbons tend to increase the selectivity loss, while the gradient in the oxygen concentration improves the selectivity of the intermediate product. Therefore, a low oxygen concentration compared to that towards the hydrocarbons is desired to avoid a negative effect on the product selectivity.

### 3.1.2 Increase of particle size and catalyst mass to account for the reduced activity

If the reduced particle effectiveness is compensated for by an increase of the catalyst mass, such that the axial oxygen concentration profile approaches the values of the original catalyst mass without intraparticle mass transfer limitations (Figure 6a), the integral effect of the mass transfer limitations on the styrene selectivity turns out to be slightly positive (Figure 6b).

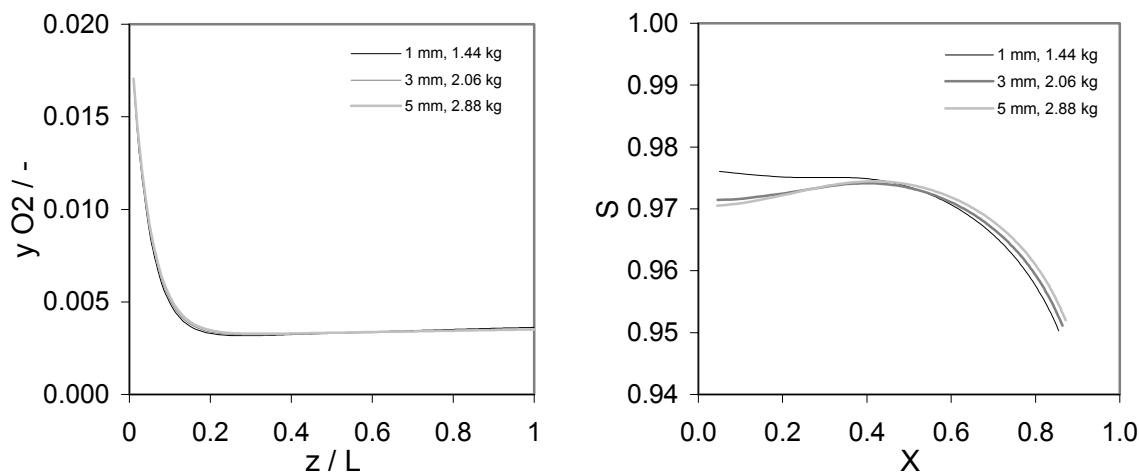


Figure 6. Influence of the particle size on the (a) the axial oxygen concentration profile and (b) selectivity – conversion – plot.

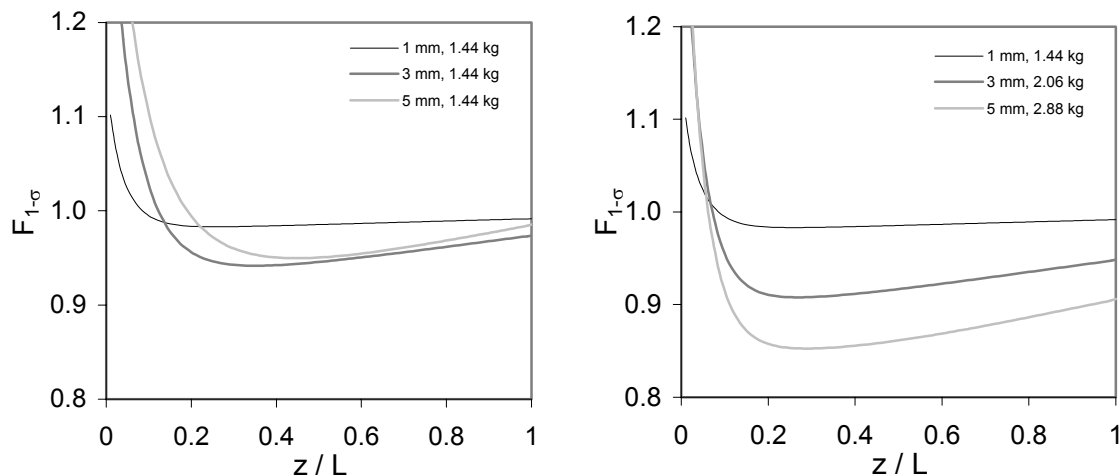


Figure 7. Comparison of the axial profile of the local selectivity loss for three different particle sizes (a) at constant catalyst mass and (b) increased catalyst mass to compensate for activity loss.

The positive effect of intraparticle oxygen concentration gradients surpasses the negative effect of the hydrocarbon gradients, such that the selectivity loss ( $F_{1-\sigma} > 1$ ) in the first 10-20 % of reactor is more than compensated for by selectivity improvements in the remaining section of the reactor. Figure 7 shows a comparison of the selectivity factor  $F_{1-\sigma}$  as function of the axial position and the modified Thiele-modulus for both situations with a fixed catalyst mass and with catalyst masses increased with the particle diameter. The decrease of the oxygen concentration, i.e. the increase of the ratio of hydrocarbon to oxygen concentrations, results in a decrease of  $F_{1-\sigma}$  over the entire length of the reactor. Concluding, it can be stated that the effect of intraparticle mass transfer limitations can be fully compensated for by an - even though significant - increase of the catalyst mass without negative effects on the styrene selectivity.

### 3.2 Transport from the membrane

In the following the influence of mass transfer limitations from the membrane wall to the core of the packed bed on the integral performance of a PBMR of industrial size is evaluated. Intraparticle mass transport effects are neglected here. The 2-D model including the Navier-Stokes equations was used in this study, where 100 grid cells were used in the axial and 80 in the radial direction, and the time step size was  $1 \cdot 10^{-4}$  s for the flow model and  $1 \cdot 10^{-2}$  s for the reaction model. For the selection of the reactor dimensions typical diameters and length of multi-tubular reactors were chosen, i.e. 10-40 mm diameter and 2-12 m length (Ullmann's encyclopedia, 1996). An important design criterion is the pressure drop over the packed bed. A relative short membrane with a relatively large tube radius should be chosen. Furthermore, selecting large catalyst particles helps reducing the pressure drop. Therefore, somewhat larger particle sizes were chosen compared to the discussion of the intraparticle effects. The chosen particle diameters 4 and 8 mm – giving pressure drops of 0.24 bar and 0.63 bar respectively – result in small tube-to-particle diameter ratios of  $d_t/d_p=10$  and  $d_t/d_p=5$ , affecting the average bed porosity. In order to be able to compare the calculation results the catalyst density was adjusted in such a way that the overall amount of catalyst in the reactor was kept constant. The model parameters have been listed in Table 5.

Table 5. Additional model parameters for the study of mass transfer limitations from the membrane to the center of the packed bed for the ODH of ethylbenzene. The feed flows were kept the same as before (see Table 4).

Reactor length	L	2 m
Membrane tube diameter	$d_t$	0.04 m
Catalyst mass	$m_{cat}$	1.44 kg
Particle diameter	$d_p$	4 ( $d_t/d_p=10$ ), 8 ( $d_t/d_p=5$ )
Bed porosity	$\varepsilon$	0.41, 0.448
Catalyst density	$\rho_{cat}$	971, 1038 kg / m <sup>3</sup>



The radial mass transport increases linearly with the particle diameter according to Eqn. 12 for the turbulent dispersion coefficient. Thus, the increase of the particle size in order to reduce the pressure drop also helps reducing mass transfer problems from the membrane wall to the center of the packed bed. A modified Thiele modulus is formulated for the transport of oxygen from the membrane surface to the center of the packed bed:

$$\phi'' = \frac{d_t}{4} \sqrt{\frac{\left(\frac{0.5+1}{2} 0.5 r_1 + \frac{1+1}{2} (10.5 r_2 + 10 r_3)\right) m_{cat} / \left((\pi/4) d_t^2 L\right)}{D_r (p_{O_2} / RT)}} \quad (18)$$

The axially averaged values for the modified Thiele modulus for the two selected particle diameters are about  $\phi''=0.93$  ( $d_t/d_p=5$ ) and  $\phi''=1.4$  ( $d_t/d_p=10$ ). For the chosen process parameters the effect of transport limitations is very small as can be seen in Figure 8a, in spite of the fact that clear radial oxygen concentration profiles are formed with ratios between the concentration of oxygen at the membrane wall and in the center of the catalyst bed of 2.3 ( $d_t/d_p=5$ ) and 4.7 ( $d_t/d_p=10$ ) (see Figure 8b). Nevertheless, the axial profile of the radially averaged oxygen concentrations is hardly effected.

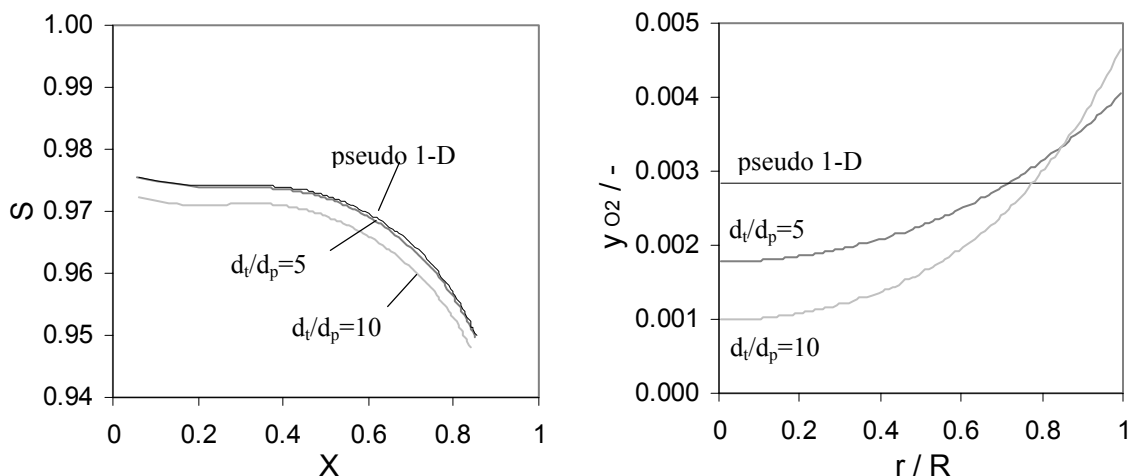


Figure 8. Influence of the membrane tube diameter on (a) the selectivity – conversion – plot and (b) the radial oxygen concentration profile at the axial position  $z/L=0.5$ .

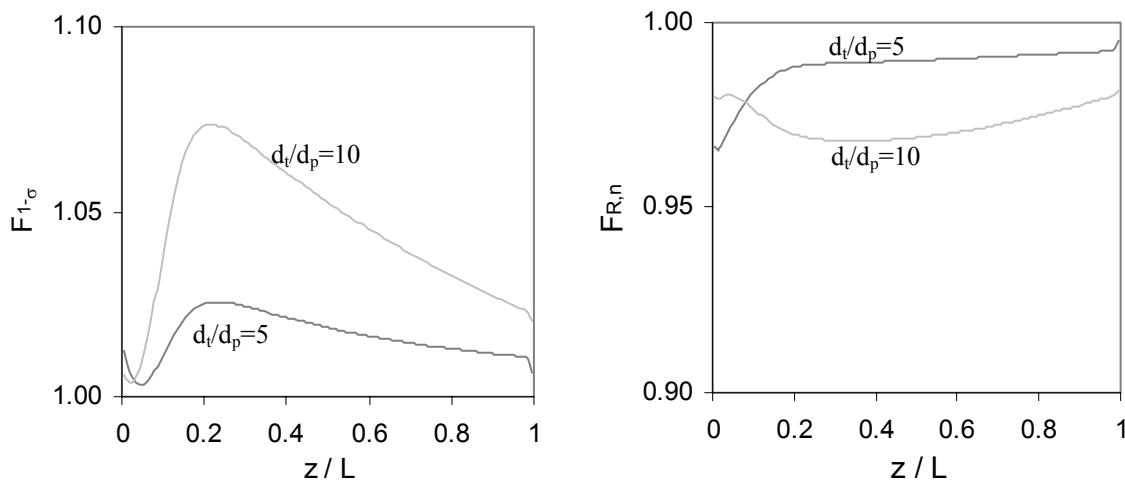


Figure 9. Influence of the membrane tube diameter on (a) the selectivity loss and (b) the relative average reaction rate of the primary reaction as function of the axial position in the reactor.

In Figure 9 the intrinsic effect of the mass transfer limitation on the selectivity factor and the relative average rate of the reaction forming the target product (defined analogously to Eqn. 17) are presented. For the given reaction orders in oxygen and for the fixed membrane flow assumed for the PBMR model radial concentration profiles result in a selectivity loss ( $F_{1,\sigma} > 1$ ). Opposite to the intraparticle transport limitations both the gradients in the oxygen concentration and in the hydrocarbon concentrations decrease the selectivity towards the intermediate product styrene.

Obviously, the particle effectiveness for catalyst diameters of 4 mm and 8 mm respectively should be considered in the design of the PBMR. Because of the reduced particle efficiencies the PBMR has to be operated at lower volumetric flow rates of premixed and distributive feed. At lower flow rates the size of the catalyst particles can be reduced at the same pressure drop. Thus, both intraparticle and membrane-to-center mass transfer limitations may become significant. Either way, the ODH of ethylbenzene to styrene cannot be operated in a PBMR at maximal productivity, but will be at least decreased by about a half, which is the effectiveness factor of a catalyst particle of  $d_p = 5$  mm.

### 3.3 Summary

For the ODH of ethylbenzene to styrene an oxygen concentration of about  $y_{O_2} = 0.05$  in a PBMR is sufficient to outperform the ODH in a packed bed reactor with premixed feed, yet to compete with the SMART process the average oxygen concentration must be an order of magnitude smaller ( $y_{O_2} \approx 0.005$ ).

Intraparticle mass transfer limitations can be compensated for by an increase of the catalyst mass, i.e. by a factor of about 2 for  $d_p = 5$  mm, without styrene selectivity losses.

In first instance – neglecting intraparticle effects – the effect of transport limitations from the membrane wall to the center of the packed bed is small in a reactor of industrial scale, if dimensioned under the design criterion of a small pressure drop. However, the required particle size is large, so that the catalyst effectiveness is expected to be small. The flow rates have to be decreased and the particle size increased. To design an industrial PBMR for the ODH of ethylbenzene a heterogeneous, 2-D model is advised.

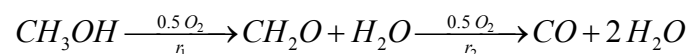
## 4 OXIDATIVE DEHYDROGENATION OF METHANOL

Formaldehyde is one of the most versatile chemicals. It is irreplaceable as a C1 building block and an intermediate in the manufacture of e.g. polyurethane and polyester plastics, resins, resin coatings, dyes, tanning agents, dispersion and plastics precursors, and so on (Ullmann's, 1996).

Formaldehyde is produced industrially from methanol by partial oxidation and dehydrogenation in the presence of air. The reaction can be either catalyzed by  $MoO_3/Fe_2O_3$  (250-400°C) at excess of oxygen, or by silver (600-720°C) under oxygen deficiency. The latter case seems more attractive to test the concept of distributive oxygen addition.

V. Diakov, A. Varma and co-workers investigated the oxidative dehydrogenation of methanol over Fe-Mo oxide catalyst in a packed-bed membrane reactor (Diakov et al. 2001, 2002a, 2002b). The standard composition of the reaction gases was 6 % methanol and 20 % oxygen similar to the composition in industrial processes. Variation of these concentrations showed (Diakov et al. 2001) that high methanol concentrations and low oxygen concentrations favor the selectivity of formaldehyde. Experimental results have been presented that show that at high conversions better selectivities were obtained in a PBMR with distributive addition of oxygen compared with a FBR with the same total feed composition.

Diakov et al. (2002b) presented a kinetic investigation of the oxidative conversion of methanol in the temperature range of 200 to 250 °C. The reaction mechanism is described by a simple consecutive reaction path:



The kinetic investigation involved the variation of the overall feed concentrations of oxygen (5-20 %) and methanol (2-10 %) and the temperature (200-250°C). It can be concluded that the experiments were conducted in most cases with an excess of oxygen. The best fit of the experimental results was achieved with the following rate expressions:

$$r_1 = 0.0048 \exp(-17630(1/T - 1/485)) p_{CH_3OH}^{0.5} \quad [\text{bar / s}] \quad (19)$$

$$r_2 = \frac{2.9 \exp(-17630(1/T - 1/485)) p_{CH_2O} p_{O_2}}{[1 + 3.9 \exp(-5920(1/T - 1/485)) p_{O_2}]^2} \quad [\text{bar / s}] \quad (20)$$

Diakov et al. performed their kinetic investigation just below the temperature range of industrial practice. According to their kinetics the order in oxygen of the consecutive reaction decreases with increasing temperature, and with it the potential profit of distributive oxygen feeding. For high temperatures above the range of the kinetic investigation the rate of the undesired combustion reaction decreases with increasing oxygen concentrations (300°C: from  $p_{O_2}=0.04$ ), and a high reaction order in oxygen for the consecutive reaction can be found only for very low partial pressures of oxygen. This could also provide an explanation for the fact that the industrial process is operated with an excess of oxygen.

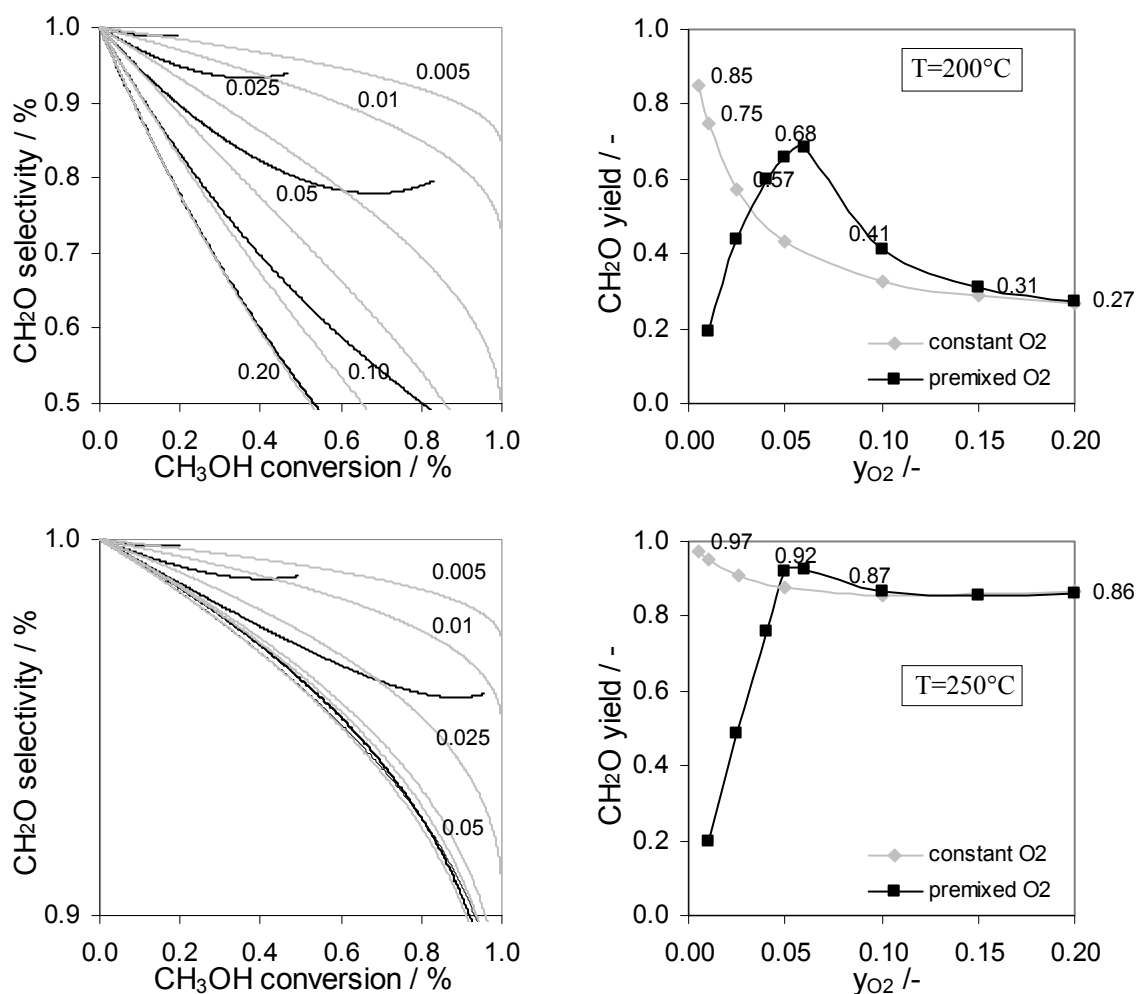


Figure 10. Comparison of FBR and PBMR (with axially constant oxygen concentration) in (a) selectivity-conversion-plot and (b) maximum formaldehyde yield for the reaction temperatures 200 and 250°C.

In Figure 10 the performance of a packed bed reactor with premixed feed (FBR) and the PBMR with axially constant oxygen concentration are compared under ideal conditions, i.e. no axial mixing and no mass transfer limitations. With increasing reaction temperature the maximum yield improves for both the FBR and PBMR. While the absolute value of the yield improvement in the PBMR reduces with increasing temperature, the relative improvement (related to the part of methanol not converted to formaldehyde) does not.

Low oxygen concentrations, i.e. below about  $y_{O_2}=0.01$ , are required to achieve with the PBMR higher formaldehyde yields than with the FBR. Note that in the experimental kinetic investigation by Diakov et al. (2002b) overall inlet oxygen concentrations above  $y_{O_2}=0.05$  were used. Provided that the reaction rate expression is still valid down to  $y_{O_2}=0.01$ , significant yield improvements can be realized in a PBMR.

In the following section the effect of mass transfer limitations on the performance of the PBMR for the ODH of methanol will be evaluated. The determination of an optimal distribution pattern of oxygen between the premixed and the distributive flow to achieve a maximum product yield (as presented for the ODH of ethylbenzene in Section 0) is not possible due to the zero order in oxygen for the primary reaction. The decrease of the oxygen concentration has no consequences for the formation rate of the target product, and thus an infinitely small oxygen concentration in the reactor is the theoretical, but impractical optimum. Therefore, a somewhat arbitrary chosen distribution pattern was chosen with an oxygen concentration in the premixed feed of  $y_{O_2,0}=0.01$  and a distributive flow that does not result in higher oxygen concentrations. For numerical stability, the primary reaction was rendered to a first order in oxygen below a concentration of  $y_{O_2}=10^{-5}$ .

#### 4.1 Intraparticle transport

The effects of intraparticle mass transfer limitations were studied for the ODH of methanol using the model parameters listed in Table 6.

Table 6. Model parameters for the study of intraparticle mass transfer limitations effects for the ODH of methanol.

Reactor length	L	2.1 m
Membrane tube diameter	$d_t$	0.04 m
Particle diameter	$d_p$	1, 3, 5 mm
Interphase mass transfer coefficient	$k_s$	1 m / s
Reactor pressure and temperature	$p, T$	1.013 bar, 550 K
Premixed feed:	volumetric flow	$\Phi_{V,0}$ 9 m <sup>3</sup> (STP) / h
	mole fraction of reactant A	$y_{EB,0}$ 0.1
	mole fraction of oxygen	$y_{O_2,0}$ 0.01
Distributed feed:	volumetric flow	$\Phi_{V,distr}$ 2.25 m <sup>3</sup> (STP) / h
	mole fraction of oxygen	$y_{O_2,distr}$ 0.2

STP: 1.013 bar and 298 K

The target of the formaldehyde process with a PBMR was set at a conversion of 98 % or higher and a formaldehyde yield exceeding 92 %. The high methanol conversions make it difficult to obtain oxygen concentrations below that of methanol near the end of the reactor, especially for a constant distribution of the distributed feed. As a consequence of the zero-order in oxygen of the first reaction and the low ratio of the rates of secondary and primary reaction, the oxygen consumption rate is almost exclusively a function of the methanol concentration and decreases continuously over the length of the reactor. This results in strong gradients in the axial concentration profiles of oxygen (see  $d_p=1$ mm in Figure 11a).

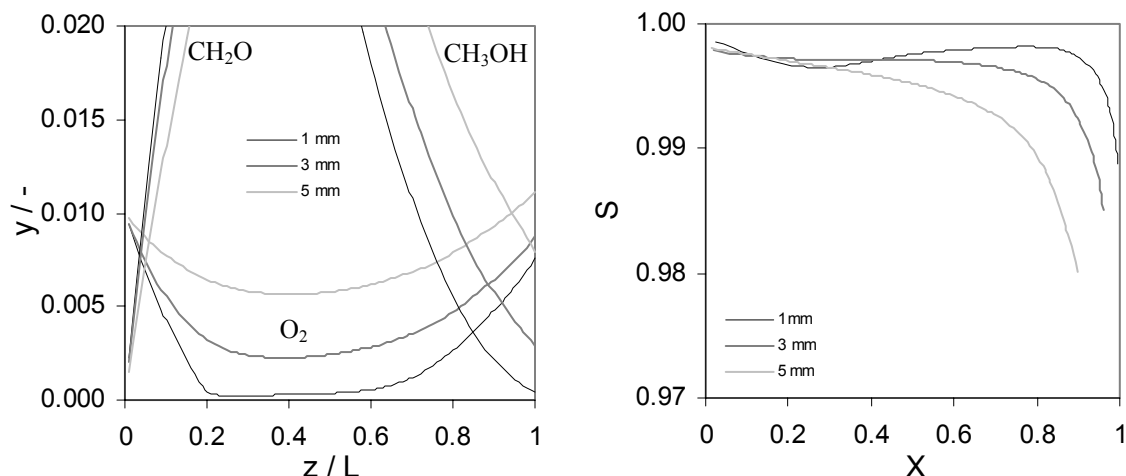


Figure 11. Influence of the particle size on the (a) the axial concentration profiles and (b) selectivity – conversion – plot at 250°C.

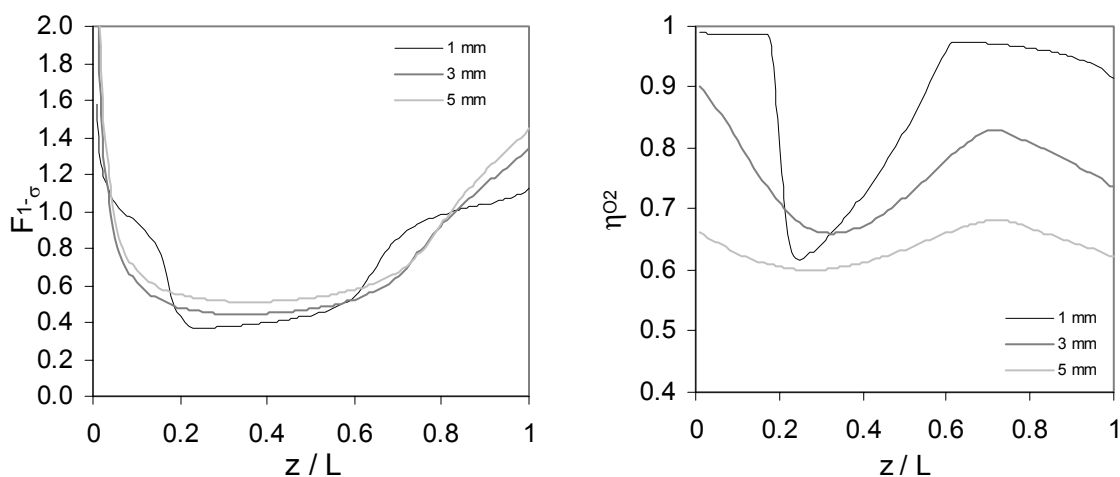


Figure 12. (a) Local selectivity loss and (b) local particle effectiveness towards oxygen consumption as a function of the axial position of the catalyst particle in the bed for three different particle diameters.

However, while the reaction rate is unaffected by the oxygen concentrations, the rate of diffusive transport inside the particle decreases linearly with the oxygen concentration. Therefore, the modified Thiele-modulus  $\phi'$  changes significantly over the reactor length, especially for  $d_p=1\text{mm}$ , where the oxygen concentration changes over two orders of magnitude very rapidly, as can be seen from the strong drop of  $F_{1-\sigma}$  and  $\eta_{\text{O}_2}$  in Figure 12. Different zones of the PBMR show totally different effects of intraparticle mass transfer limitations on the intrinsic selectivity and particle effectiveness.

The conversion-selectivity plot in Figure 11b shows that intraparticle mass transfer limitations have a strong effect already for a particle diameter of  $d_p=3\text{mm}$  for the reaction conditions considered here. Through an increase of the reactor volume by 35 % ( $d_p=3\text{mm}$ ) and 100 % ( $d_p=5\text{mm}$ ) respectively, the same methanol conversion is obtained as for  $d_p=1\text{mm}$ , and the integral selectivity losses can be reduced (Kürten, 2003).

Note that the oxygen concentration increases strongly towards the reactor end caused by the axially constant permeation flux, while the methanol concentration is small due to the high conversion. This oxygen concentration increase strongly enhances the consecutive reaction reducing the formaldehyde selectivity. Thus a

better PBMR performance is expected with an axially decreasing oxygen concentration flux, especially close to the reactor outlet.

#### 4.2 PBMR with linearly decreasing membrane flux

In the following the calculations for the intraparticle effects were repeated with a linearly decreasing membrane flux. (Additionally, the distributive flow is reduced to  $\Phi_{V,distr}=1.8 \text{ m}^3/\text{h}$ .) By this means, it can be avoided that the oxygen concentration exceeds the concentration of methanol near the reactor exit (see Figure 13b), and consequently the previously observed strong selectivity loss in this region of the reactor is prevented.

The linear decreasing distribution ensures as well that the integral effect of the intraparticle mass transfer limitations on the formaldehyde selectivity is positive, provided that the effectiveness loss is compensated for by an increase of the catalyst mass (i.e. reactor size) (see Figure 14b).

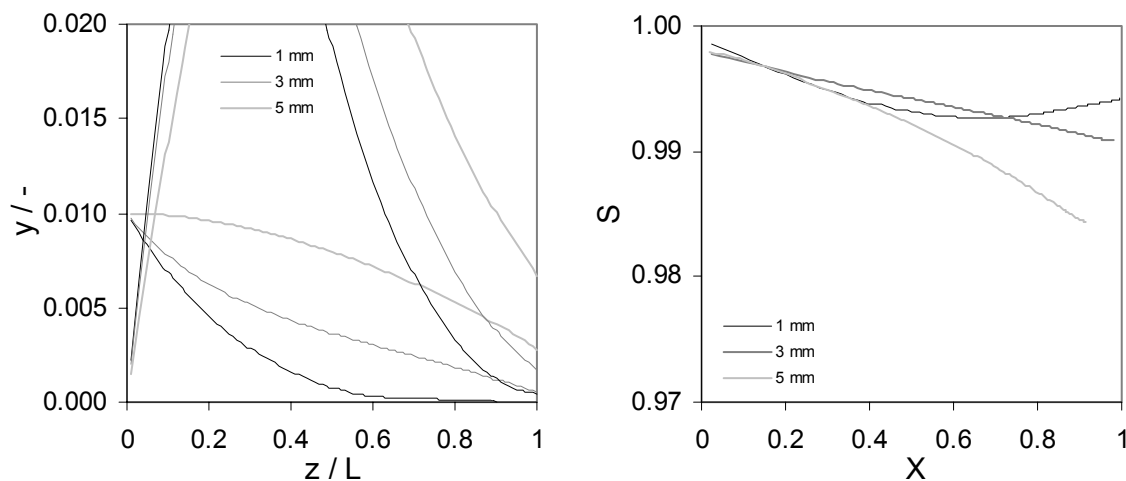


Figure 13. Influence of the particle size on the (a) the axial concentration profiles and (b) selectivity – conversion – plot for a linearly decreasing membrane flux.

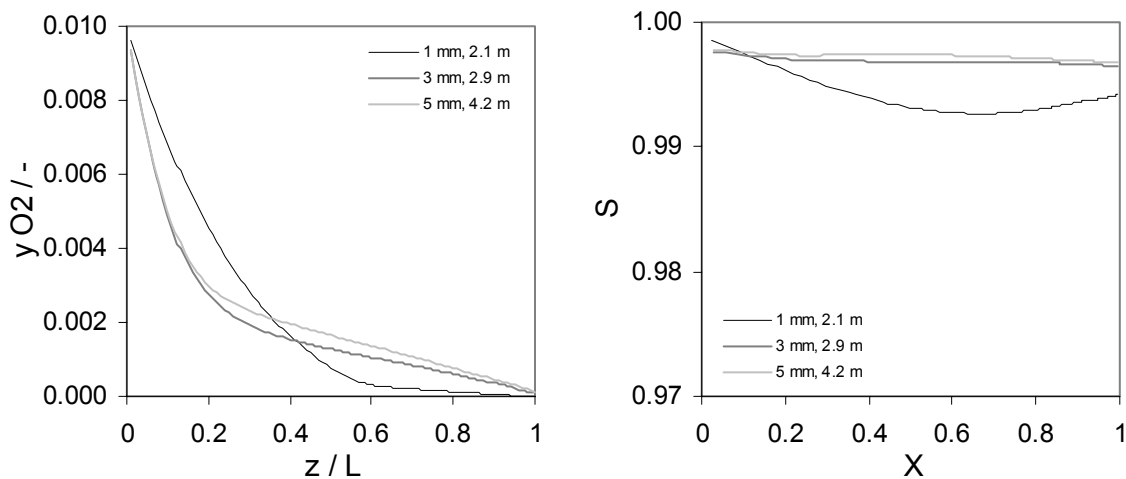


Figure 14. Influence of the particle size on the (a) the axial concentration profiles and (b) selectivity – conversion – plot for a linearly decreasing membrane flux.

### 4.3 Transport from the membrane

For the evaluation of the transport effect from the membrane to the center of the packed bed intraparticle effects were neglected. The parameters are the same as in Table 6 besides the particle diameter, which is chosen to obtain the following diameter ratios  $d_t/d_p=20, 10$  and  $5$  respectively (see Table 7). Due to the modified Thiele-moduli up to about  $\phi''=6$ , very strong radial oxygen concentration profiles develop in the middle zone of the PBMR from  $z/L=0.2$  to  $0.6$  with oxygen depletion in the center of the packed bed, as shown in Figure 15.

Table 7. Additional model parameters for the study of mass transfer limitations from the membrane to the center of the packed bed for the ODH of methanol.

Particle diameter	$d_p$	2 ( $d_t/d_p=20$ ), 4 (10), 8 (5)
Bed porosity	$\varepsilon$	0.39, 0.41, 0.448

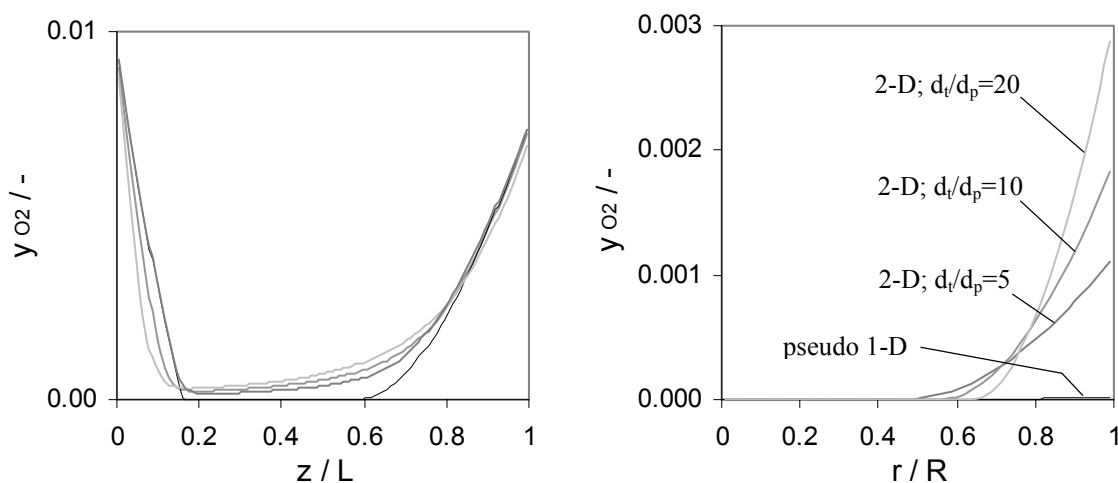


Figure 15. Influence of the particle diameter on the (a) the axial oxygen concentration profile and (b) the radial oxygen concentration profile at the axial position  $z/L=0.5$ .

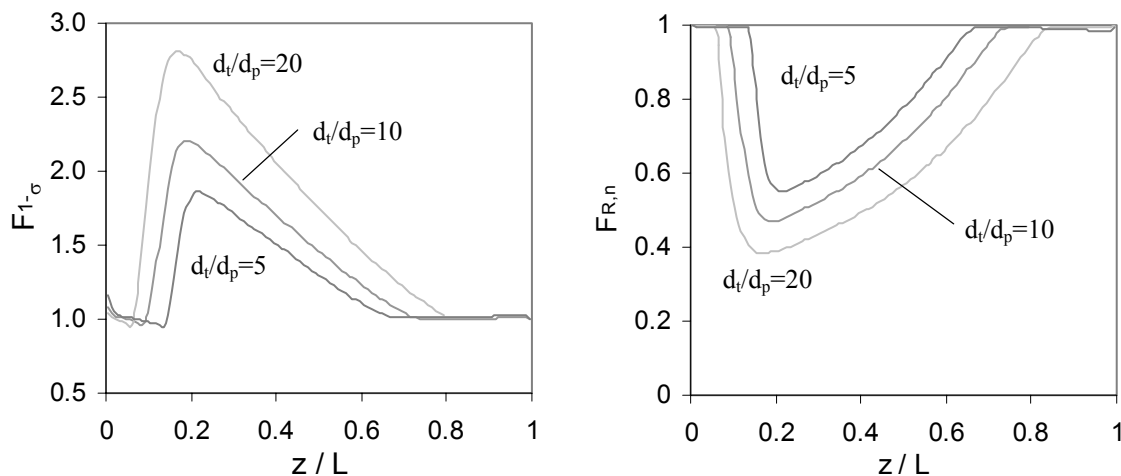


Figure 16. Influence of the particle diameter on (a) the selectivity loss and (b) the relative average reaction rate of the primary reaction.

As shown in Figure 16 there is a strong effect of the transport limitations on the intrinsic selectivity and the average reaction rate of the primary reaction. Thus, the selectivity-conversion plot Figure 17 shows a significant effect on the formaldehyde selectivity - but the effect on the conversion seems to be negligible.

This apparent discrepancy is simply explained by the difference in the pressure drop resulting from the change in the particle diameter from 1.42 bar ( $d_t/d_p=20$ ) to 0.68 bar ( $d_t/d_p=10$ ) and 0.27 bar ( $d_t/d_p=5$ ). The selectivity decreases for increasing  $d_t/d_p$  ratios, showing the negative effect of radial mass transfer limitations.

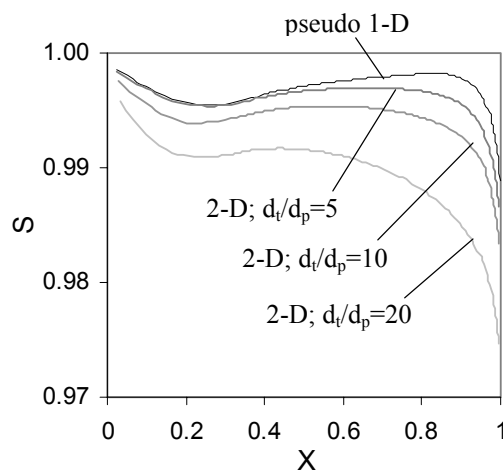


Figure 17. Influence of the particle diameter on the selectivity – conversion – plot.

#### 4.4 Operation at high methanol concentrations

A PBMR offers the possibility to operate partial oxidation processes at overall feed compositions, which are not feasible in a FBR due to flammability limits. If the industrial process is operated with undiluted feed ( $y_{O_2}$  about 0.2) the methanol concentration must be limited at about  $y_{CH_3OH}=0.06$ . The productivity of the process can be almost doubled if the oxygen concentration is decreased below  $y_{O_2}=0.1$ , e.g. by recycling the reactor outlet flow, which is enriched in nitrogen (Centi et al., 2002), due to the shift in the explosion limits.

In a PBMR the overall concentration of methanol can be doubled. Feed concentrations of  $y_{CH_3OH,0}=0.8$  (rest air:  $y_{O_2,0}=0.04$ ) with a distributive flow of about  $\Phi_{V,distr}/\Phi_{V,0}=2.2$  would result in an overall feed composition for a FBR of  $y_{CH_3OH,0}=0.267$  and  $y_{O_2,0}=0.144$ , which is within the flammability region for a FBR.

However, the reaction orders in the hydrocarbons are not in favor of an increase of the methanol concentration with respect to the product selectivity, according to the kinetic investigation by Diakov et al. (2002b). The productivity increases according to a square root function of the methanol concentration, and due to the fact that the consecutive reaction yield shows a first order dependency with respect to the formaldehyde concentration, the maximum product yield (at the same oxygen concentration level) decreases with increasing hydrocarbon concentration. To achieve the same conversion level as for low methanol concentrations the volumetric flow of the premixed feed has to be reduced by a factor of 5, which results in a productivity improvement of about 60 % (8:5). However, the selectivity is just 95 % compared to above 98 % calculated for the low methanol concentration.

Furthermore, the initial temperature rise increases and the particle effectiveness near the reactor inlet decreases due to the high methanol concentrations, so that an increase of the initial methanol concentrations is not attractive at least for a PBMR. Possibly, it is a promising option to increase the productivity utilizing a fluidized bed membrane reactor because of the better temperature control and the possibility to use very small particles.

#### 4.5 Summary

It was shown that the ODH of methanol to formaldehyde can be improved in a PBMR resulting in product yields above 92 %. However, due to the low local oxygen concentrations (high modified Thiele-moduli) the effect of mass transfer limitations is considerable. The catalyst particles and the packed bed will locally be used inefficiently with a corresponding reduced productivity of the PBMR. For optimal product yields a (linearly) decreasing membrane flux is advised.

The model calculations were based on the kinetics of Diakov et al. (2002b), which assumes a zero reaction order in oxygen for the primary reaction. However, the concentrations in the PBMR are locally very low. It is not unlikely that the zero-order in oxygen does not hold at very low oxygen concentrations, but gradually changes to a



first order dependency (e.g. following a Langmuir-Hinshelwood type kinetics). Yet, very high selectivities can already be realized if the rate of the primary reaction is almost constant down to an oxygen concentration of about  $y_{O_2}=0.01$ .

## 5 CONCLUSIONS

The distributive feeding of oxygen was studied for the ODH of ethylbenzene to styrene and of methanol to formaldehyde. For both reaction systems it was shown that by means of distributive feeding of oxygen higher product yields can be obtained than for pure premixed oxygen feeding. For low oxygen concentrations the PBMR can compete with industrial processes. Yet, an experimental verification is required if the assumed reaction kinetics, viz. the reaction orders in oxygen, are valid at these low oxygen concentrations.

For the investigation of mass transfer limitations inside the catalyst particle and from the membrane to the center of the packed bed a one-dimensional heterogeneous model and a two-dimensional, pseudo-homogeneous model including hydrodynamics were developed. The intrinsic effect of intraparticle mass transport limitations on the selectivity can be positive if the oxygen concentration is small compare to those of the hydrocarbons. Therefore, negative effects of intraparticle transport limitations on the PBMR performance can be avoided, provided that the decreased catalyst activity is compensated for by an increase of the catalyst mass. The effect of membrane-to-center mass transport limitations on the ODH of ethylbenzene in a industrial scale reactor is small, because pressure drop requirements limit the applicable tube-to-particle diameter ratio. In case of the ODH of methanol locally very low oxygen concentrations eventuate strong effects of membrane-to-center mass transfer limitations. For industrial scale PBMR a two-dimensional reactor model is advised if the modified Thiele-modulus  $\phi''$  significantly exceeds values of 1.

The investigation of the mass transfer effects in PBMRs is an essential first step for the development of a true PBMR-model. Due to mass transfer limitations a large part of the catalyst in a PBMR is not used efficiently; the effectiveness of the catalyst packing is strongly reduced. This influences the distribution of the activity over the length of the packed bed, and thus the distribution of the released reaction heat. Mass transfer limitation can even be made use of. If the rate of the primary reaction is independent of the oxygen concentration (see ODH of methanol), the initial temperature rise can be decreased with an oxygen-free feed.

## NOTATION

$a$	specific surface area [ $m^2/m^3$ ]
$d$	diameter [m]
$D_{eff}$	effective mass diffusion coefficient [ $m^2/s$ ]
$D_r^t$	radial mass transport coefficient due to turbulent dispersion [ $m^2/s$ ]
$F$	factor by which a reaction rate or selectivity is increased due to mass transport limitations [-]
$k_s$	gas-solid mass transfer coefficient [m/s]
$L$	length of the packed bed [m]
$M_i$	molecular mass of component i [kg/mol]
$m_{cat}$	catalyst mass [kg]
$nr$	number of reactions
$n_{s,i}$	interfacial mass flux of component i [kg / m <sup>2</sup> s]
$p$	pressure [bar]
$r_j$	rate of reaction j [mol / g <sub>cat</sub> s]
$R_i$	rate of reactive consumption of component i in nr reactions ( $= \sum_{j=1}^{nr} \nu_{ij} \Gamma_j$ ) [mol / g <sub>cat</sub> s]
$S$	source term [kg / m <sup>3</sup> s]
$S$	selectivity [-]
$T$	temperature [K],[°C]
$u$	supervicial gas velocity ( $\varepsilon v$ ) [m / s]

$v$	interstitial gas velocity [m / s]
$X$	conversion [-]
$y$	molar fraction [-]

## Greek letters

$\varepsilon$	porosity [-]
$\eta$	effectiveness factor [-]
$\lambda_g$	gas bulk viscosity [kg / m s]
$\mu_g$	gas shear viscosity [kg / m s]
$\nu$	stoichiometric coefficient
$\rho$	density [kg / m <sup>3</sup> ]
$\sigma$	intrinsic selectivity of the target product [-]
$\tau$	tortuosity [-]
$\overline{\tau}_g$	gas phase stress tensor [kg / m s]
$\phi_{m,distr}$	added mass flow per reactor volume [kg / m <sup>3</sup> s]
$\Phi_m$	mass flow [kg / s]
$\Phi_V$	volumetric flow [m <sup>3</sup> / s] or [ml / min]
$\omega$	mass fraction [-]

## Subscripts

$0$	at the reactor inlet / base case
$cat$	catalyst
$distr$	distributed
$EB$	ethylbenzene
$g$	gas
$O_2$	oxygen
$p$	particle
$t$	tube

## Dimensionless numbers

$\phi'$	modified Thiele-modulus
$\phi''$	modified Thiele-modulus
$\langle x \rangle$	represents the spatial average of variable $x$
$\bar{x}$	represents the vector representation of variable $x$

## REFERENCES

- Bird, R.B., Stewart, W.E., Lightfoot, E.N., in "Transport phenomena", John Wiley & Sons, New York (1960).
- Brinkman, H.C., Appl. Sci. Research, Vol. A1, 27-34 (1947).
- Cavani, F., Trifirò, F., "Review Alternative processes for the production of styrene", Applied Catalysis, Vol. A 133, 219-239 (1995).
- Centi, G., Cavani, F., Trifirò, F., "Selective Oxidation by heterogeneous catalysis", Kluwer Academic / Plenum Publishers, New York (2002).

Diakov, V., Larfarga, D., Varma, A., "Methanol oxidative dehydrogenation in a catalytic packed-bed membrane reactor", *Catalysis Today*, Vol. 67, 159 – 167 (2001).

Diakov, V., Varma, A., "Reactant distribution by inert membrane enhances packed-bed reactor stability", *Chem. Eng. Sci.*, Vol. 57, 1099 – 1105 (2002a).

Diakov, V., Blackwell, B., Varma, A., "Methanol oxidative dehydrogenation in a catalytic packed-bed membrane reactor: experiments and model", *Chem. Eng. Sci.*, Vol. 57, 1563 – 1569 (2002b).

Fuller, E.N., Schettler, P.D., Giddings, J.C., "A new method for prediction of binary gas-phase diffusion coefficients", *Ind. Eng. Chem.*, Vol. 58, 19 (1966).

Gerhartz, W., Yamamoto, Y.S., Chambell, F.T., Pfefferkorn, R., Rounsaville, J.F., "Ullmann's encyclopedia of industrial chemistry", 5<sup>th</sup> edition, VHC, Weinheim (1985-1996).

Gunn, D.J., "Axial and radial dispersion in fixed beds", *Chem. Eng. Sci.*, Vol. 42, 363-373 (1987).

Kürten, U., "Modeling of packed bed membrane reactors: Impact of oxygen distribution on conversion and selectivity in partial oxidation systems", Ph.D. Thesis, Twente University, Enschede, The Netherlands (2003).

Hsieh, H.P., "Inorganic membranes for separation and reaction", Elsevier, Amsterdam (1996).

Mears, D.E., "Tests for transport limitations in experimental catalytic reactors", *Ind. Eng. Chem. Process Des. Develop.*, Vol. 10, 541-547 (1971).

Patankar, S.V., "Numerical heat transfer and fluid flow", McGraw-Hill, New York (1980).

Press, W.H., Flannery, B.P., Teukolsky, S.A., Vetterling, W.T., "Numerical recipes in Pascal – The art of scientific computing", Cambridge University Press (1989).

Reid, R.C., Prausnitz, J.M., Poling, B.E., "The properties of gases and liquids", McGraw-Hill Book Company, New York (1988).

Saracco, G., Neomagus, H.W.J.P., Versteeg, G.F., van Swaaij, W.P.M., "High-temperature membrane reactors: potentials and problems", *Chem. Eng. Sci.*, Vol. 54, 1997-2017 (1999).

Shakhnovich, G.V., Belomestnykh, I.P., Nekrasov, N.V., Kostyukovsky, M.M., Kiperman, S.L., "Kinetics of ethylbenzene oxidative dehydrogenation to styrene over vanadia/magnesia catalyst", *Applied Catalysis*, Vol. 12, 23-34 (1984).

Tsotsas E., Schlünder, E.U., "Some remarks on channelling and on radial dispersion in packed beds", *Chem. Eng. Sci.*, Vol. 43, 1200-1203 (1988).

Watzemberger, O., Ströfer, E., Anderlohr, A., "Unsteady-state oxidative dehydrogenation of ethylbenzene to form styrene", *Chem. Eng. Technol.*, Vol. 21, 659-662 (1999).

Westerterp, K.R., Swaaij, W.P.M van, Beenackers, A.A.C.M., "Chemical reactor design and operation", John Wiley & Sons, Chichester, (1984).

Wilke, C.R., "Diffusional properties of multicomponent gases", *Chemical Engineering Progress*, Vol. 92, 1 (1950).

## Appendix A: Estimation of the effective diffusion coefficient

A semi-empirical correlation for the binary diffusion coefficients in a gas mixture was given by Fuller et al. (1966).

$$D_{ij} = 10^{-3} \frac{T^{1.75} \sqrt{1/M_i + 1/M_j}}{p \left( \sqrt[3]{\sum_k V_{ki}} + \sqrt[3]{\sum_k V_{kj}} \right)^2} \text{ [m}^2 \text{ / s]} \quad (\text{A.1})$$

with temperature  $T$  in K, pressure  $p$  in atmosphere, molecular mass  $M$  in g/mol. The atomic diffusion volumes  $V_{ij}$  can be found in e.g. Reid et al. (1988).

The molecular diffusion coefficient is approximated with the equation proposed by Wilke (1950)

$$D_{m,i} = (1 - y_i) \left/ \sum_{\substack{j=1 \\ j \neq i}}^n \frac{y_j}{D_{ij}} \right. \quad (\text{A.2})$$

Finally, the effective diffusion coefficient is calculated with

$$D_{\text{eff},i} = \frac{\varepsilon}{\tau} D_{m,i} \quad (\text{A.3})$$